Synthetic Metals, 52 (1992) 201–211

Analysis of the infrared conductivity of the organic superconductor α-(BEDT-TTF)$_2$(NH$_4$)Hg(NCS)$_4$

M. Dressel and J. E. Eldridge
Department of Physics, University of British Columbia, Vancouver, BC, V6T 1Z1 (Canada)

H. Hau Wang, Urs Geiser and Jack M. Williams
Chemistry and Materials Science Divisions, Argonne National Laboratory, Argonne, IL 60439 (USA)

(Received February 6, 1992; accepted May 12, 1992)

Abstract

An optical study of the α phase superconducting compound, α-(ET)$_2$(NH$_4$)Hg(NCS)$_4$, has been performed. The absolute reflectivity of a deuterated crystal has been measured as a function of temperature and polarization, from which the conductivity was obtained. The overall shapes of these spectra are discussed and compared with those obtained from compounds of different phases. In particular we were able to perform a Drude fit of the low-temperature conductivity for one polarization, rather than of the reflectivity dip. The plasma frequency and damping were extracted and these yielded a reasonable effective mass and mean free path. The isotopic vibrational frequency shifts were obtained by repeating the measurements on a protonated sample, which was, however, too small to provide absolute data. The vibrational features are assigned and discussed.

Introduction

The first popular BEDT-TTF (usually abbreviated to ET) radical ion salt was α-(ET)$_2$I$_3$ [1], which was superceded by many superconductors of this family, for example, β-(ET)$_2$I$_3$ (T_c = 1.1 K) [2], β-(ET)$_2$AuI$_2$ (T_c = 5 K) [3], κ-(ET)$_2$[Cu(NCS)$_2$] (T_c = 10.4 K) [4] and κ-(ET)$_2$Cu[N(CN)$_2$]Br (T_c = 11.6 K) [5]. Various efforts to observe ambient-pressure superconductivity in an α-phase ET salt like α-(ET)$_2$I$_3$ by doping [6] or in related compounds such as α-(ET)$_2$IBr$_2$ have failed. Tempering of α-(ET)$_2$I$_3$ at 75 °C for several days leads to a superconducting crystal (T_c = 8 K), but the structure has changed to α_t, which is similar to the β phase, both crystallographically and in its physical behaviour [7]. Figure 1 shows planes of ET molecules in the α, β and κ phases.

The relatively high transition temperatures of κ-(ET)$_2$[Cu(NCS)$_2$] and κ-(ET)$_2$Cu[N(CN)$_2$]Br may have been obtained by increasing the size of the polymeric anion acceptors. Similarly, by extending the two-component system to a three-component system (donor; anion + cation = acceptor), the first

0379-6779/92/$5.00

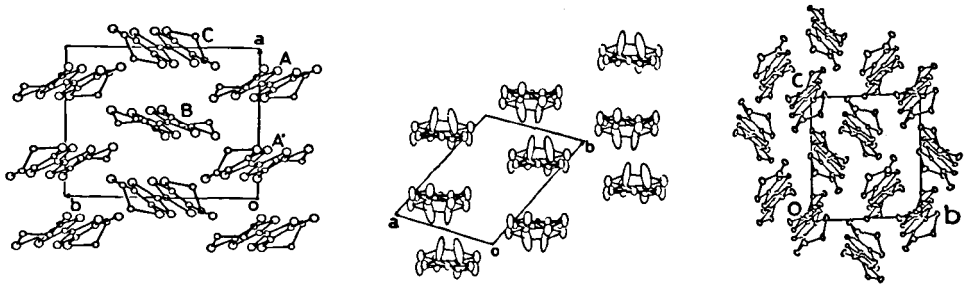

Fig. 1. Planes containing the ET molecules are shown here for the α (left), β (middle) and κ (right) phases. The ET molecules are oriented with their long axis approximately perpendicular to the planes. There are differences between the stack displacements and orientations of molecules in different stacks.

ambient-pressure ET superconductor in the α phase was eventually found: α-$(ET)_2(NH_4)Hg(NCS)_4$ with $T_c = 0.8$ K [8].

$(ET)_2(NH_4)Hg(NCS)_4$ is isostructural to $(ET)_2KHg(NCS)_4$, which is triclinic with a $P\bar{1}$ space group and $Z = 2$ [8, 9]. It crystallizes with the flat face parallel to the highly conducting ab plane [8, 10]. The ET molecules form stacks of two kinds along the a direction. One chain contains parallel ET molecules, while the second one has molecules which are tilted 6.6° with respect to their stack neighbour, and 82.3° and 75.6° with respect to the parallel molecules in the other stack.

$(ET)_2(NH_4)Hg(NCS)_4$ has a very high metallic conductivity, rising from between 100 and 400 $(\Omega\ cm)^{-1}$ at room temperature to a value approximately 100 times greater at 4.2 K [11], although Wang *et al.* [8] reported much smaller values. This is higher than the values typically seen in the ET salts and may be due to the lack of formation of strong dimers (see Discussion Section). The onset of superconductivity is near 1.15 K and the midpoint is at 0.8 K [8]. Recently reported measurements of the specific heat in an applied magnetic field also indicate the presence of the superconducting energy gap at 0.8 K [12]. The Fermi surface of the K salt has been calculated by a tight-binding method and found to be two-dimensional [13]. Large Shubnikov–de Haas oscillations were observed with a period corresponding to the extreme orbit area of 13% of the first Brillouin zone [10].

We are aware of no previously published optical investigations of $(ET)_2(NH_4)Hg(NCS)_4$. Because of the structural similarities, the optical properties may resemble those of α-$(ET)_2I_3$, on which there have been many studies [14–19]. In these, the optical conductivity was found to be fairly two-dimensional, but stronger in the polarization with the electric field perpendicular to the stacks. This is because, in an α-phase crystal, the network of strong interstack sulfur–sulfur contacts lead to a high conductivity in that direction. Vibronically induced intramolecular vibrations were also observed and discussed at some length [17]. Below 135 K, of course, α-$(ET)_2I_3$ becomes a semiconductor and we cannot compare the low-temperature spectra with those which we have obtained. β-$(ET)_2I_3$, on the other hand, remains metallic down to its superconducting transition at 1.4 K and several

optical studies have been reported [14–16, 20–22], but this phase produces a much more one-dimensional optical response, as would be expected (see Fig. 1). Other β-phase compounds such as β-$(ET)_2AuI_2$ and β-$(ET)_2I_2Br$ have also been studied optically [23], as well as a so-called α-phase compound with a different structure and stoichiometry, α-$(ET)_3(ReO_4)_2$ [18].

We have recently reported the infrared optical properties of three κ-phase superconductors, starting with κ-$(ET)_2[Cu(NCS)_2]$ [24, 25] and following with κ-$(ET)_2Cu[N(CN)_2]Br$ [26] and κ-$(ET)_2Cu[N(CN)_2]Cl$ [27]. For the first compound, spectra were measured as a function of temperature and polarization for both the protonated and deuterated material, allowing us to make reasonable assignments of the many vibrational features. We found, for the ET molecule, a predominance of vibronically activated a_g modes and normally active b_{2u} modes. One of these latter, $\nu_{49}(b_{2u})$, near 880 cm^{-1}, is very strong and has consistently been mis-assigned to $\nu_7(a_g)$ in other studies. In all three compounds we observed an interplay of oscillator strength between the interband and intraband electronic responses as the temperature was lowered.

This work reports the spectra of both protonated and deuterated α-$(ET)_2(NH_4)Hg(NCS)_4$ in order to compare both the electronic and vibrational features of an α-phase superconductor with those of some κ-phase compounds, which have a much higher T_c.

Experimental

The absolute reflectivity was measured from only the deuterated crystal, prepared at the Argonne National Laboratory, which had a fairly good surface of 1.5×1 mm^2 and was about 0.4 mm thick. The protonated sample was small and its spectra were used for vibrational assignments only. The orientation of the deuterated sample was determined by X-ray transmission through a thin end. It was highly twinned through its thickness but we were able to reflect from a predominantly single-crystal surface layer. It was glued with epoxy cement to two gold braids, each consisting of eight strands of 0.025 mm wire, and the length of the braided wires from the sample to the copper mount was approximately 1 mm. This was attached to the cold finger of an Air-Products Heli-tran refrigerator. The beam-splitters and detectors used in the far-infrared, mid-infrared and near-infrared ranges of the Bruker IFS 113V Fourier spectrometer were the same as those previously reported [24, 26]. Details of the reflectivity module have also been published [28].

Mid- and far-infrared reflectivity spectra were recorded at 300, 200, 100, 50 and 6.5 K for both polarizations on the first cooling cycle of the deuterated crystal. As a consistency check, the measurements were repeated on the second cooling cycle with a smaller beam size and a fresh aluminum mirror. The reproducibility was $\pm 3\%$. Below 80 cm^{-1} (300 K) and 250 cm^{-1} (for temperatures below 300 K due to the presence of a CsI vacuum window), the reflectivity data were extrapolated to unity at zero frequency, using the standard Drude law ($R = 1 - a\omega^{1/2}$), for the Kramers–Kronig analysis.

Results

Figure 2 shows the reflectivity up to 5000 cm^{-1} for $E\|b$ (perpendicular to the stacks) at 300, 100 and 6.5 K. The spectra obtained at 50 and 200 K have been omitted for clarity, but they fit between the three displayed. Figure 3 shows only the 300 and 6.5 K $E\|a$ (parallel to the stacks) reflectivity, since while the other temperature spectra fall between these two in the far-

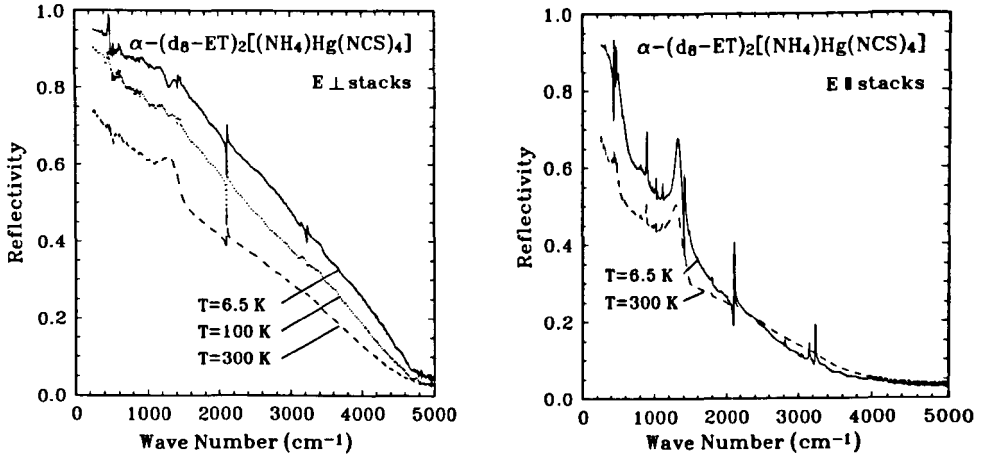

Fig. 2. Reflectivity of the deuterated form of the title compound at three indicated temperatures for $E\|b$.

Fig. 3. Reflectivity of the deuterated form of the title compound at two indicated temperatures for $E\|a$.

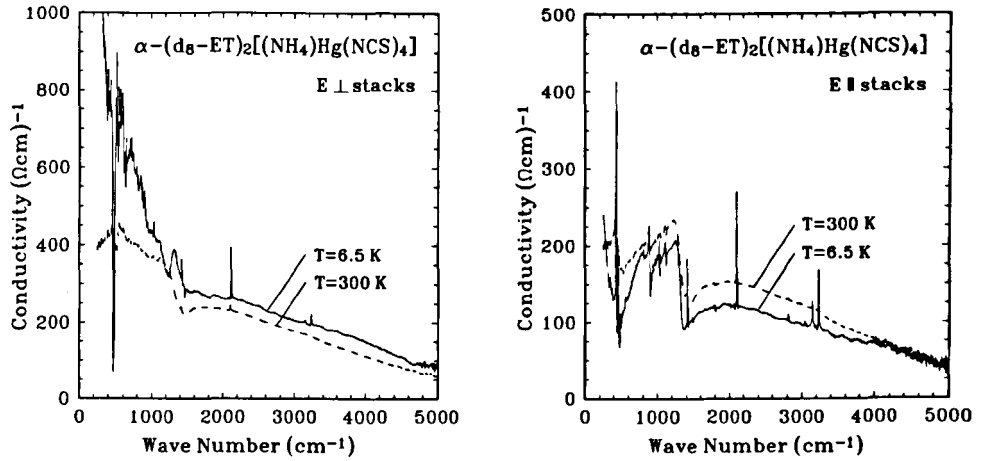

Fig. 4. Conductivity of the deuterated form of the title compound at two indicated temperatures for $E\|b$.

Fig. 5. Conductivity of the deuterated form of the title compound at two indicated temperatures for $E\|a$.

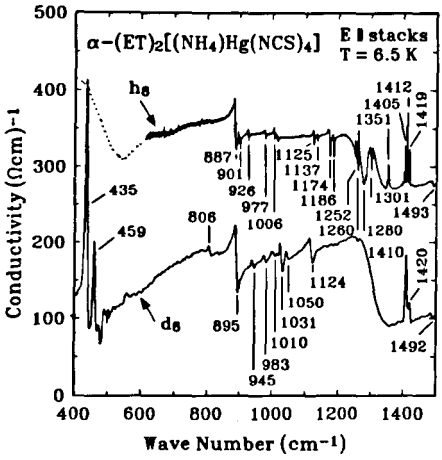

Fig. 6. Expanded portion of the low-temperature conductivity spectrum of the protonated compound (upper trace, which has been displaced by 200 $(\Omega\ cm)^{-1}$ for clarity) and of the deuterated compound (lower trace, corresponding to the ordinate scale). The upper trace below 600 cm^{-1} was very noisy due to the small crystal size. The resolution is 0.5 cm^{-1} (h_8) and 1.0 cm^{-1} (d_8).

infrared region, they show little temperature dependence above 2000 cm^{-1}. Figure 4 shows the conductivity for $\boldsymbol{E}\|\boldsymbol{b}$, obtained after a Kramers–Kronig analysis, for the two extreme temperatures. Figure 5 does likewise for $\boldsymbol{E}\|\boldsymbol{a}$. Figure 6 shows an expanded portion of the $\boldsymbol{E}\|\boldsymbol{a}$ conductivity spectra at 6.5 K of both the protonated and deuterated compound. This region contains most of the observed intramolecular vibrational modes of the ET molecule. The resolution is 0.5 cm^{-1} (h_8) and 1.0 cm^{-1} (d_8). The peaks or dips (marked with an asterisk in Table 1) have been labeled with their wave number (cm^{-1}).

Discussion

Electronic transitions

The conductivity spectra obtained at 300 K in Figs. 4 and 5 agree with those reported for α-$(ET)_2I_3$ (e.g. ref. 18) in as much as the conductivity perpendicular to the ET molecule stacks is greater than that parallel to the stacks. The overall shapes, however, differ from those of α-$(ET)_2I_3$ mainly because of the much higher d.c. conductivity (cf. 100–400 $(\Omega\ cm)^{-1}$ for $(ET)_2(NH_4)Hg(NCS)_4$ versus 20–60 $(\Omega\ cm)^{-1}$ for $(ET)_2I_3$), to which our far-infrared conductivities extrapolate. The vibronic interactions at 1300 cm^{-1} and below are also more prominent for $\boldsymbol{E}$ parallel to the stacks (in Fig. 5) than in Fig. 4. This is in marked contrast to the room-temperature results of α-$(ET)_2I_3$.

In our studies of the κ-phase materials we observed broad peaks in the mid-infrared conductivity, near 2200 cm^{-1} for one polarization and between 3000 and 4000 cm^{-1} for the other. We correlated these qualitatively with

TABLE 1

Frequencies and assignment of the vibrational features for protonated and deuterated α-$(ET)_2(NH_4)Hg(NCS)_4$. Sample temperatures were at 10 K. All frequencies are in cm^{-1}. δ is the observed isotope shift

E‖*a*			*E*‖*b*			Assignment[b]	Calc. freq.[c]	Calc. shift[d]
h_8[a]	d_8[a]	δ	h_8[a]	d_8[a]	δ			
4212*w						2ν(CN)		
3229s	3230s	+1	3236w	3230w	−6	$\nu_3(f_2)NH_4^+$	3145*	
3142m	3141m	−1	3141w	3141vw	0			
2812vw	2814w	+2				$2\nu_4(f_2)NH_4^+$		
2113w			2124w			ν(CN)	2074*	
2111s			2120w					
2110m			2116m					
2105s	2106s	+1	2113vs	2113s	0			
			2107m					
1789*vw	1783vw	−6				$2\nu_{49}(b_{2u})$		
1493*w	1492*w	−1				$\nu_2(a_g)$	1465	0
1419m	1420m	+1	1419s			$\nu_4(f_2)NH_4^+$	1400*	
1412s	1410s	−2	1411w					
1408w								
1405m	1124*s	−281	1405vw			$\nu_4(a_g)$	1421	−274
1402w			1401vw					
1351m	983*m	−368	1352m			$\nu_{45}(b_{2u})$	1409	−345
1308*w			1309*vw			$\nu_5(a_g)$	1287	−257
1301*m	1050*m	−251	1303*m					
1295*vw			1288*s	1030m	−258			
1285*w			1282*vw					
1280*vs	1031*s	−249						
1260*s	1010*m	−250	1262*m					
1252*m								

1200–1350	1250–1350		1200–1350	1250–1400	$\nu_3(a_g)$	1427	0
1186*m 1174*m			1185m 1174m		$\nu_{14}(a_u)$	1182	−310
1137*w 1125*m	806	−331	 1124w		$\nu_{67}(b_{3u})$	1152	−335
1016*w 1014*vw 1012*vw 1009*vw 1006*m	945*m	−71	 1009w 1005w		$\nu_{47}(b_{2u})$	1025	−74
977*m					$\nu_6(a_g)$	979	−66
926*m 922*w					$\nu_{48}(b_{2u})$	917	−15
901*m					$\nu_7(a_g)$	896	−108
896*w 887*vs 883*m	895*vs	+8			$\nu_{49}(b_{2u})$	898	−1
	459s 435vs			480*vs 468vs	$\nu_9(a_g)$? $\nu_{10}(a_g)$?	508 489	0 −1

[a] vs = very strong; s = strong; m = medium; w = weak; vw = very weak. The asterisk denotes anti-resonance.
[b] The assignment for multiplets is listed opposite the first component only.
[c] Ref. 31.
[d] Ref. 32.
[e] Ref. 33.

vertical interband transitions between occupied and unoccupied bands throughout the Brillouin zone [24]. No such maximum is seen in Fig. 4, however, where $\boldsymbol{E}$ is perpendicular to the stacks, even though the band structure for $(ET)_2[(NH_4)Hg(NCS)_4]$ is very similar to that for $(ET)_2Cu(NCS)_2$ [29].

Tajima *et al.* [21] have interpreted the conductivity spectra of β-$(ET)_2I_3$ in a similar fashion and have calculated both the interband and intraband contributions to the conductivity as a function of polarization, using the band structure of Mori *et al.* [30]. They obtained qualitative agreement with experiment and also found that the strength of the interband transitions depends strongly on the dimerization of the ET molecules. This is because the mid-infrared interband transitions are essentially due to the formation of charge-transfer excitons confined to nearest neighbors. Similar calculations have been performed by Yakushi *et al.* [18] for α-$(ET)_2I_3$. It would appear, therefore, that the accentuation of the far-infrared intraband conductivity in Fig. 4 follows from the sum rule and is at the expense of the interband conductivity which has decreased due to the lack of dimers in the $\boldsymbol{E}$ perpendicular to the stacks polarization.

While we have not performed detailed calculations of the conductivity using the results of band structure calculations, we show in Fig. 7 a fit of the low-temperature conductivity (with $\boldsymbol{E}$ perpendicular to the stacks) to two functions, namely, a Drude response in the far-infrared, combined with a heavily damped harmonic oscillator to represent the broad mid-infrared strength. The parameters for the Drude fit are $\omega_p = 7000$ cm^{-1} and $\gamma = 700$ cm^{-1}. This value of ω_p is similar to that usually found in organic conductors (e.g. ref. 34), and assuming two holes from four ET molecules per unit cell, with a unit cell volume of 2008 Å^3, giving $n = 9.96 \times 10^{20}$ per cm^3, one obtains an effective mass of $1.8m_e$, which is also a typical value found from

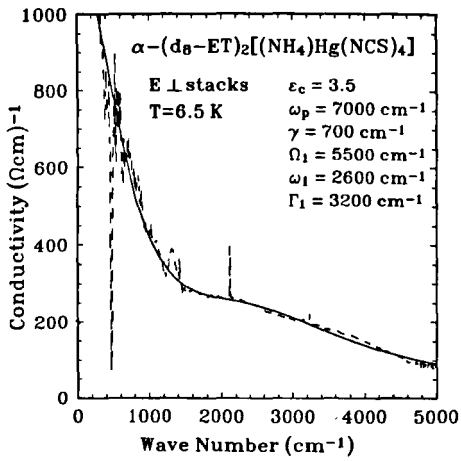

Fig. 7. Conductivity at 6.5 K from Fig. 4 compared with a fit to a Drude term with $\epsilon_c = 3.5$, $\omega_p = 7000$ cm^{-1} and $\gamma = 700$ cm^{-1}, combined with a damped oscillator at 2600 cm^{-1}, with damping of 3200 cm^{-1} and oscillator strength of 5500 cm^{-1}, to reproduce the mid-infrared response.

Drude fits and magnetic measurements. We show this result because we believe that this is the first time that such parameters have been obtained from a fit of the conductivity rather than of the dip in the reflectivity. At room temperature the conductivity is usually too low for any fit and at low temperatures, if there is not a phase transition to a semiconductor, then the zero-frequency peak may be much narrower than in Fig. 4. For example the 12 K half-width for $(ET)_2Cu(NCS)_2$ is ~ 40 cm^{-1} [34] which requires a large effective mass of $8m_e$. The damping of 700 cm^{-1} is less than that usually found from a reflectivity dip. It corresponds to a scattering time, τ, of 5×10^{-14} s. From the electronic band structure calculated by Whangbo [29], the slope at the Fermi level gives a Fermi velocity of $\sim 0.2\times10^8$ cm/s. The mean free path $\Lambda = v_F\tau$ is then obtained as ~ 100 Å which is a reasonable value. One sees, however, that the wide Drude peak in Figs. 4 and 7 is not present in the other polarization (Fig. 5) which would therefore also require a heavy effective mass. This leads one to speculate whether there might be a connection between this heavy effective mass, in those materials which conduct at low temperatures, and the strongly interacting $\nu_3(a_g)$ phonon which is due to dimers. This phonon, near 1300 cm^{-1}, is weak in Figs. 4 and 7 in which the Drude response is broad but prominent in Fig. 5 where the response is narrow and the effective mass large.

Vibrational assignments

Figure 6 shows the detailed high-resolution vibrational spectra between 400 and 1500 cm^{-1} of both the protonated and deuterated compounds for $E\|a$ (parallel to the stacks). Table 1 lists the observed features in the low-temperature spectra of both polarizations, along with our experimental isotope shifts, assuming we have correctly identified the corresponding features in both spectra and our assignments based on the calculated frequencies and isotope shifts. An asterisk indicates the frequency of a dip in an anti-resonance, rather than a peak. Not all of the minor features in Table 1 are labeled in Fig. 6. The phonon feature which dominates the spectra of most ET salts is the vibronically activated, totally symmetric $\nu_3(a_g)$ internal mode of the ET radical cation involving the central C=C bond, calculated by Kozlev *et al.* [31] to occur at 1427 cm^{-1} (see, for example, refs. 17, 20 and 24). In Fig. 6, however, this mode has become a broad shoulder extending from 1200 to 1350 cm^{-1}, which is clearly a result of the absence of strong dimers in the α phase. On the other hand, the strongest feature, at 435 cm^{-1} in the deuterated spectrum of Fig. 6, along with the 459 cm^{-1} companion, is still either $\nu_9(a_g)$ and/or $\nu_{10}(a_g)$. (The protonated spectra were very noisy in this region, due to the small crystal size.) They occur at the same frequency as in the κ-phase compounds that we have studied [24–27]. The next largest feature is $\nu_{49}(b_{2u})$ at 895 cm^{-1} (d_8). It has a much stronger Fano shape for $E\|a$ than is seen in the κ-phase compounds. While only the totally symmetric (a_g) modes of the gerade species have the correct symmetry to interact with the electronic continuum and become infrared active, it is of course possible for the normally infrared-active ungerade modes to interact also with the

electronic background. $\nu_{49}(b_{2u})$ has been described in ref. 25 where we speculated that it is strongly involved in the creation of charge-transfer excitons between differently oriented ET molecules. $\nu_5(a_g)$, involving the ethylene groups, is again prominent as its many split components interfere with $\nu_3(a_g)$ between 1252 and 1308 cm^{-1}. It is possible that this mode is split into seven components. Two strong vibrations of the NH_4^+ tetrahedron are observed: $\nu_3(f_2)$ with two components near 3200 cm^{-1} (see Figs. 2–5), and $\nu_4(f_2)$ with up to five components near 1412 cm^{-1} (see Fig. 6). The sharp CN lines are again seen near 2100 cm^{-1}.

The remaining assignments in Table 1 are more speculative, but since the vibrational structure is stronger and more detailed for this compound than we observed for the κ-phase compounds, a few reassignments are suggested. Comparing Table 1 with the corresponding table for κ-$(ET)_2[Cu(NCS)_2]$ in ref. 24, one observes that $\nu_{45}(b_{2u})$ is present and strong here whereas it was weak and unidentified previously. The doublet at 1186 and 1174 cm^{-1} is possibly $\nu_{14}(a_u)$ rather than $\nu_{67}(b_{3u})$, which may be the lower doublet at 1137 and 1125 cm^{-1}. Similarly, the group around 1006 cm^{-1} is closer to the calculated frequency for $\nu_{47}(b_{2u})$, as is 977 cm^{-1} for $\nu_6(a_g)$. The other assignments are unchanged. One may also note that $\nu_1(a_g)$ is not observed here and that $\nu_2(a_g)$ is at a higher frequency than that previously observed, and that $\nu_4(a_g)$ is much stronger than it was in ref. 24.

Acknowledgements

Work at the University of British Columbia was supported by Grant No. 5-85653 from the Natural Sciences and Engineering Research Council (NSERC) of Canada. Work at Argonne National Laboratory was performed under the auspices of the Office of Basic Energy Sciences, Division of Materials Sciences, of the US Department of Energy, Contract W-31-109-Eng-38. M.D. acknowledges support from the Deutsche Forschungsgemeinschaft (DFG), Germany.

References

1 K. Bender, K. Dietz, H. Endres, H. W. Helberg, I. Hennig, H. J. Keller, H. W. Schäfer and D. Schweitzer, *Mol. Cryst. Liq. Cryst.*, *107* (1984) 45.
2 E. B. Yagubskii, I. F. Shchegolev, V. N. Laukhin, P. A. Kononovich, M. V. Karatsovnik, A. V. Zvarykina and L. I. Buravov, *JETP Lett.*, *39* (1984) 12.
3 J. M. Williams, H. H. Wang, M. A. Beno, U. Geiser, M. A. Firestone, K. S. Webb, L. Nuñez, G. W. Crabtree K. D. Carlson, L. J. Azevedo, J. F. Kwak and J. E. Schirber, *Physica B*, *135* (1985) 520.
4 H. Urayama, H. Yamochi, G. Saito, K. Nozawa, T. Sugano, M. Kinoshita, S. Sato, K. Oshima, A. Kawamoto and J. Tanaka, *Chem. Lett.*, (1988) 55.
5 A. M. Kini, U. Geiser, H. H. Wang, K. D. Carlson, J. M. Williams, W. K. Kwok, K. G. Vandervoort, J. E. Thompson, D. L. Stupka, D. Jung and M.-H. Whangbo, *Inorg. Chem.*, *29* (1990) 2555.

6 E. B. Yagubskii, I. F. Shchegolev, V. N. Laukhin, R. P. Shibaeva, E. E. Kostyuchenko, A. G. Khomenko, Yu. V. Sushko and A. V. Zvarykina, *JETP Lett.*, *40* (1984) 1201; W. Kremer, H. W. Helberg, E. Gogu, D. Schweitzer and H. J. Keller, *Ber. Bunsenges, Phys. Chem.*, *91* (1987) 896.

7 D. Schweitzer, P. Bele, H. Brunner, E. Gogu, U. Haeberlen, I. Hennig, I. Kluts, R. Swietlik and H. J. Keller, *Z. Phys. B*, *67* (1987) 489.

8 H. H. Wang, K. D. Carlson, U. Geiser, W. K. Kwok, M. D. Vashon, J. E. Thompson, N. F. Larsen, G. D McCabe, R. S. Hulscher and J. M. Williams, *Physica C*, *166* (1990) 57.

9 M. Oshima, H. Mori, G. Saito and K. Oshima, *Chem. Lett.*, (1989) 1159.

10 T. Osada, A. Kawasumi, R. Yagi, S. Kogoshima, N. Miura, M. Oshima, H. Mori, T. Nakamura and G. Saito, *Solid State Commun.*, *75* (1990) 901.

11 H. Mori, S. Tanaka, K. Oshima, M. Oshima, G. Saito, T. Mori, Y. Maruyama and H. Inokuchi, *Solid State Commun.*, *74* (1990) 1261.

12 B. Andraka, G. R. Stewart, K. D. Carlson, H. H. Wang, M. D. Vashon and J. M. Williams, *Phys. Rev. B*, *42* (1990) 9963.

13 M. Oshima, H. Mori, G. Saito and K. Oshima, in G. Saito and S. Kagoshima (eds.), *The Physics and Chemistry of Organic Superconductors, Springer Proceedings of Physics*, Vol. 51, Springer, Berlin, 1990, p. 257.

14 B. Koch, H. P. Geserich, W. Ruppel, D. Schweitzer, K. H. Dietz and H. J. Keller, *Mol. Cryst. Liq. Cryst.*, *119* (1985) 343.

15 M. G. Kaplunov, E. B. Yaubskii, L. P. Rosenberg and Yu. G. Borodko, *Phys. Status Solidi (a)*, *89* (1985) 509.

16 T. Sugano, K. Yamada, G. Saito and M. Kinoshita, *Solid State Commun.*, *55* (1985) 137.

17 M. Meneghetti, R. Bozio and C. Pecile, *J. Phys. (Paris)*, *47* (1987) 1377.

18 K. Yakushi, H. Kanabara, H. Tajima, H. Kuroda, G. Saito and T. Mori, *Chem. Lett.*, (1987) 4251.

19 V. Želznỳ, J. Petzelt, R. Swietlik, B. P. Gorshunov, A. A. Volkov, G. V. Kozlov, D. Schweitzer and H. J. Keller, *J. Phys. (Paris)*, *51* (1990) 869.

20 C. S. Jacobsen, J. M. Williams and H. H. Wang, *Solid State Commun.*, *54* (1985) 937.

21 H. Tajima, K. Yakushi, H. Kuroda and G. Saito, *Solid State Commun.*, *56* (1985) 159.

22 H. Tajima, H. Kanbara, K. Yakushi, H. Kuroda and G. Saito, *Solid State Commun.*, *57* (1986) 911.

23 C. S. Jacobsen, D. B. Tanner, J. M. Williams, U. Geiser and H. H. Wang, *Phys. Rev. B*, *35* (1987) 9605.

24 K. Kornelsen, J. E. Eldridge, H. H. Wang and J. M. Williams, *Phys. Rev. B*, *44* (1991) 5235.

25 K. Kornelsen, J. E. Eldridge, H. H. Wang and J. M. Williams, *Solid State Commun.*, *74* (1990) 501.

26 J. E. Eldridge, K. Kornelsen, H. H. Wang, J. M. Williams, A. V. Strieby Crouch and D. M. Watkins, *Solid State Commun.*, *79* (1991) 583.

27 K. Kornelsen, J. E. Eldridge, H. H. Wang, H. A. Charlier and J. M. Williams, *Solid State Commun.*, *81* (1992) 343.

28 J. E. Eldridge and C. C. Homes, *Infrared Phys.*, *29* (1989) 143.

29 M. H. Whangbo, personal communication.

30 T. Mori, A. Kobayashi, Y. Sasaki, H. Kobayashi, G. Saito and H. Inokuchi, *Chem. Lett.*, (1984) 957.

31 M. E. Kozlov, K. I. Pokhodnia and A. A. Yurchenko, *Spectrochim. Acta, Part A*, *45* (1989) 437.

32 M. E. Kozlov, K. I. Pokhodnia and A. A. Yurchenko, *Spectrochim. Acta, Part A*, *43* (1987) 323.

33 K. Nakamoto, *Infrared and Raman Spectra of Inorganic and Coordination Compounds*, Wiley, New York, 1986.

34 K. Kornelsen, J. E. Eldridge, C. C. Homes, H. H. Wang and J. M. Williams, *Solid State Commun.*, *72* (1989) 475.